Supporting Information

Sustainable High-Pressure Homogenization of Hexagonal Boron Nitride for Triboelectric Nanogenerator: Advancing Self-Powered Environmental Monitoring in Portable Electronics

Yawar Abbas,[a,b†] Rohan B. Ambade,[c,d†] Muhammad Umair Khan,[b,e] Rui Chang,[c,d] Yahya Zweiri,[c,d] Baker Mohammad,[b,e] Dalaver Anjum,[f*] Yarjan Abdul Samad[c,g*]

[a]Center for Cyber-Physical Systems - System on Chip Lab, Khalifa University of Science & Technology, 127788, Abu Dhabi, United Arab Emirates.

[b]James Watt School of Engineering, University of Glasgow, Glasgow, G12 8QQ, UK

[c]Department of Aerospace Engineering, Khalifa University of Science & Technology, 127788, Abu Dhabi, United Arab Emirates

[d]Advanced Research and Innovation Center, Khalifa University of Science & Technology, 127788, Abu Dhabi, United Arab Emirates

[e]Department of Computer and Information Engineering, Khalifa University, Abu Dhabi 127788, UAE

[f]Department of Physics, Khalifa University of Science and Technology (KUST), P.O Box 127788, Abu Dhabi, United Arab Emirates

[g]Cambridge Graphene Center, University of Cambridge, 9 JJ Thomson Avenue, Cambridge CB3 0FA, United Kingdom

† Contributed equally to this work.

*Corresponding author: E-mail: yarjan.abdulsamad@ku.ac.ae, yy418@cam.ac.uk (Yarjan Abdul Samad)

Experimental

Preparation of 2D hBN Flakes *via* High-Pressure Homogenization Process: The schematic illustration of the designed HPH process is shown in **Scheme 1**. The AVESTIN "EmulsiFlex™-C3" was used for the HPH process. The homogenization was done by varying the process cycles (1-100). The details are discussed in **Scheme 1**.

Fabrication of Triboelectric Nanogenerator: Contact separation (CS)-mode TENG is fabricated using hBN as an electropositive material and FEP as an electronegative material. A flexible PET substrate of size 12 cm × 5 cm was taken as a base substrate, and a 4 cm × 5 cm pair of Al tapes separated by ~ 1 cm was attached to the PET substrate *via* double-sided tape. The FEP sheet of 4 cm × 5 cm is connected to the first Al tape, and hBN is spray-coated on the second Al tape. The spray-coated hBN is dried for 2 h at 60 ˚C in N_2 ambient. After completing the above process, the base substrate is folded half along its length for the tapping of electropositive and electronegative material. (a) The two copper wires were attached to Al tapes to extract open circuit voltage and short circuit current values. The open circuit voltages and short circuit current were extracted using the Rohde & Schwarz RTO1014 Oscilloscope and Keithley 4200A-SCS Parameter Analyzer, respectively. The capacitors and resistors were connected to the standard breadboards for the application part and the calculation of the power density of the TENG.

Materials Characterization: The phase of the hBN flakes was analyzed using powder X-ray diffraction (XRD, EMPYREAN) with a K-Alpha1 radiation $\lambda = 1.5405$ Å) images collected in the 2θ (twice the Bragg angle) range of 10–80° at a scan speed of 5 min^{-1}. The Raman spectroscopy was performed using a Renishaw Raman spectrometer with a 633 nm laser as the excitation source. Scanning electron microscopy (SEM, Hitachi S4800) was used to investigate the surface morphologies. Transmission electron microscopy (TEM) and high-resolution TEM (HRTEM)

were performed at an acceleration voltage of 200 kV. High angular annular dark-field scanning TEM (HAADF–STEM) images and energy-dispersive X-ray spectroscopy (EDS) maps were acquired using a JEOL JEM– ARM200F microscope operated at an acceleration voltage of 80 kV. The powdered hBN samples were dissolved in 99.99% grade ethyl alcohol for the dispersion of nanosheets. About 2 μL was directly drop-casted onto a holey carbon-coated copper grid (mesh size 300 nm) (purchased from Electron Microscopy Sciences) for 45 seconds, and the excess sample was blotted with a filter paper. Afterward, the sample containing grids was analyzed in a double aberration-corrected transmission electron microscope (TEM) of model Titan ThemisZ from ThermoFisher Scientific, which was also equipped with an energy filter of model 1069HR/K3 from Gatan, Inc. The TEM analysis of hBN nanosheets was performed by operating the microscopes at the accelerating voltage of 80 kV to cause no damage or minimum damage to samples during the data acquisition. The microscope was set to bright-field TEM (BF-TEM) with monochromator excited mode to acquire several images at different magnifications. The geometrical phase analysis (GPA) was applied to acquired high-resolution TEM (HR-TEM) images to map strain in the normal directions and demonstrate the defect-free (atomic scale pores and/or dislocations) surface of hBN samples. The composition of the hBN samples was investigated by carrying out the core-loss electron energy loss spectroscopy (EELS) analysis of samples. The core-loss EELS experiments were performed by setting the microscope in the micro-probe scanning TEM (STEM) mode. Suitable energy dispersion and shift values were selected to set the field of view of EELS spectra so that the boron, nitrogen, and oxygen energy loss edges become visible in the acquired datasets. Three-dimensional STEM-EELS datasets were acquired for the elemental maps of boron and nitrogen elements from hBN nanosheets. The composition of hBN samples was also determined quantitatively by analyzing the acquired core-loss EELS spectra

of hBN samples. Furthermore, the shape of the boron and nitrogen edges was compared with standard hBN edges to gauge the quality of the synthesized hBN nanosheets.

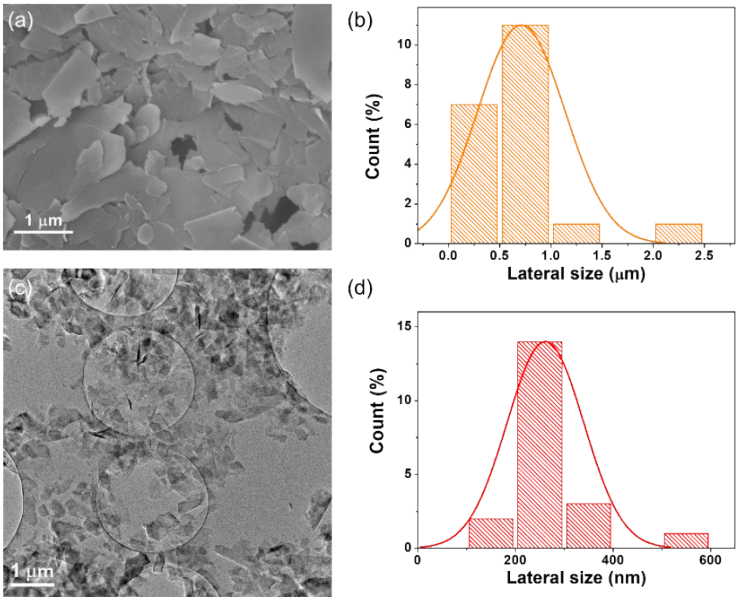

Figure S1. (a) SEM image, (b) statistical analysis of lateral size from SEM image, (c) TEM image, and (d) statistical analysis of lateral size from TEM image of the HPH-prepared 2D hBN flakes lateral size.

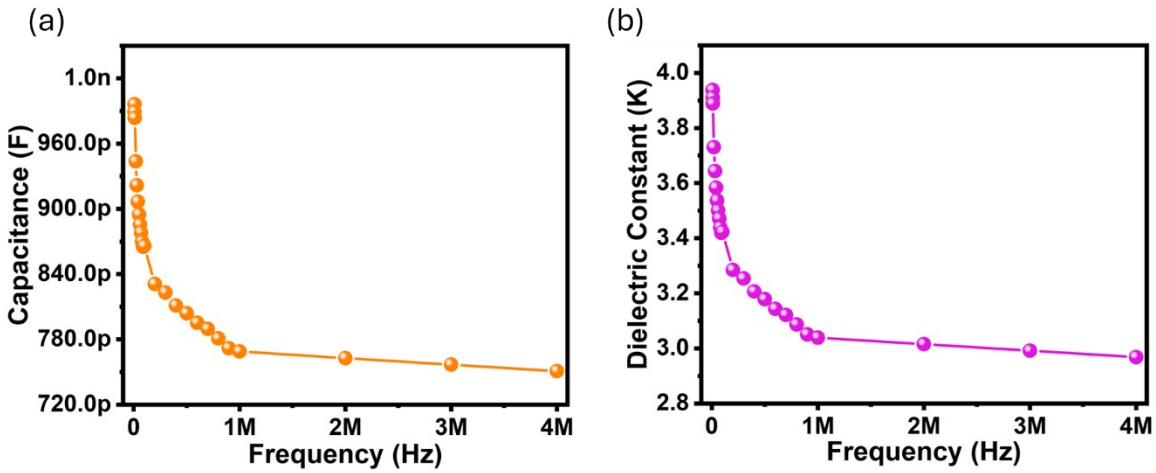

Figure S2. (a) Capacitance, and (b) dielectric measurement across frequency sweep of 8 kHz to 4 MHz for the prepared films hBN film.

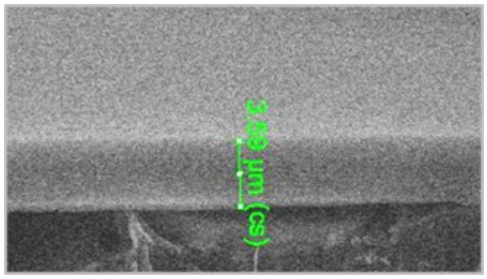

Figure S3. Cross-sectional SEM image showing the clearly defined triboelectric layer with a uniform thickness of approximately 3.5 µm, confirming precise layer deposition.

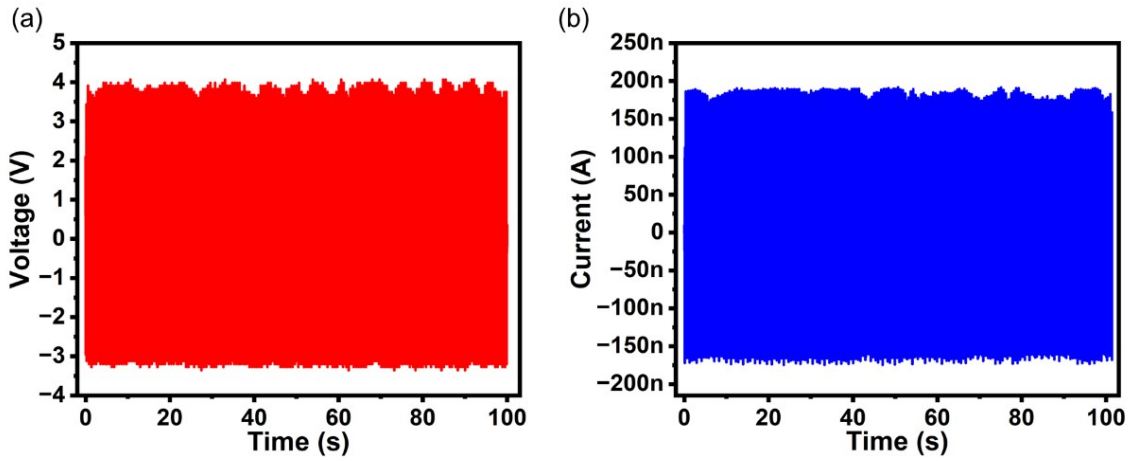

Figure S4. The piezoelectric nanogenerator based on Al/hBN/Al shows (a) open circuit voltage and (b) short circuit current.

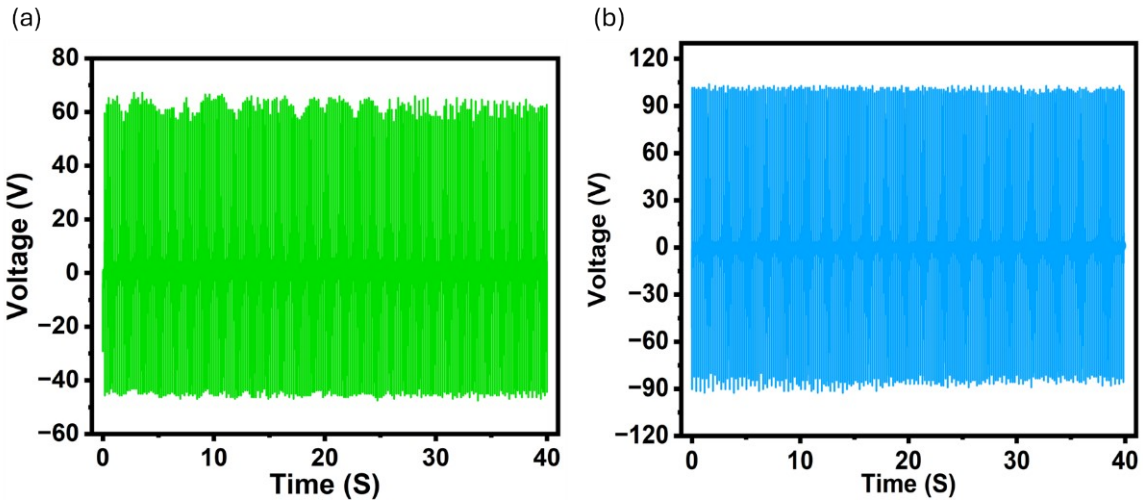

Figure S5. Comparative performance of TENG devices fabricated using (a) bulk hBN and (b) commercial hBN as triboelectric layers.

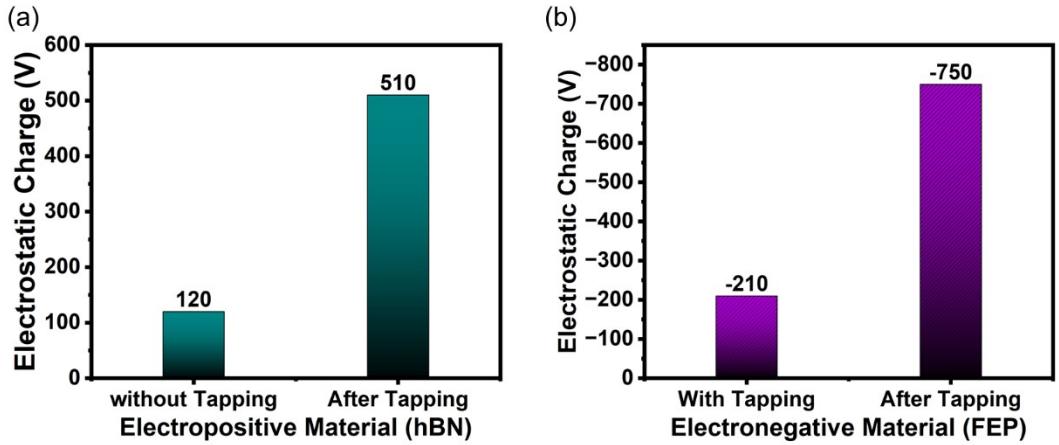

Figure S6. Electrostatic surface potential of (a) hBN and (b) FEP without and after tapping.

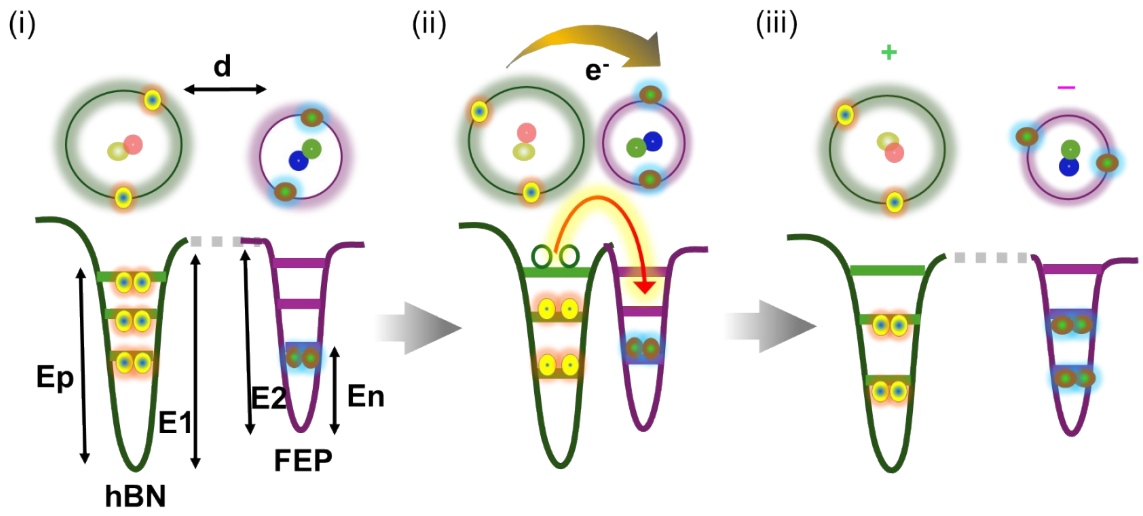

Figure S7. The electron charge transfer method.

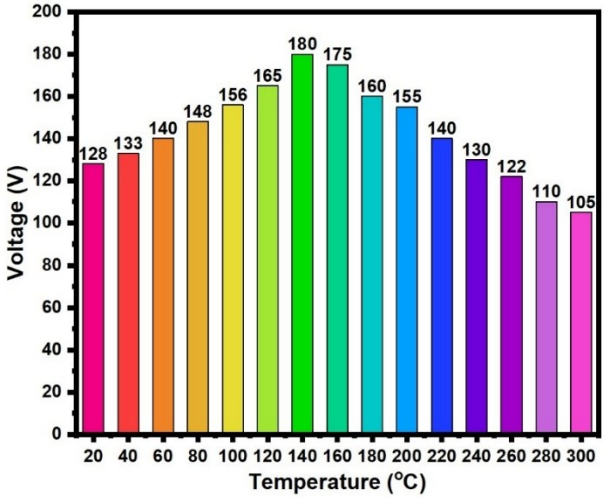

Figure S8. The dependence of open circuit voltage on the temperature.

Table S1. The comparison of the TENG performance of the scalable HPH synthesized hBN flakes with other synthesis methods of h-BN-based state-of-the-art TENGs. (h-BNNS: hexagonal boron nitride nanosheets)

Triboelectric materials	**Synthesis method**	**Voltage V_{oc} (V)**	**Short circuit current (I_{sc}) µA**	**Current density (J_{sc}) mA/m²**	**Power/Power density (P_d) W/m²**	**References**
MoS_2-hBN	Pulsed laser deposition	14.7	-	-	-	[1]
h-NNSs/ BoPET	Liquid-phase assisted exfoliation	200	-	0.48	0.14	[2]
PVDF NFs-h-BNNS	Chemical exfoliation	500	25.2	-	3.13	[3]
Polycarbonate-h-BNNS	Liquid-phase assisted exfoliation	800	-	0.78	1.36	[4]
PDMS-h-BNNS	Hydrothermal-assisted exfoliation	150	15	-	-	[5]
PVC-hBN nanosheets	Hydrothermal-assisted exfoliation	142	272	-	0.307	[6]
Plastic-hBN	Mixing annealing approach	68	6.1	-	0.46	[7]
HPH-hBN flakes	**High-pressure homogenizer (HPH)**	**135**	**17**	**-**	**18**	**This work**

References

[1] S. Parmar, A. Biswas, S. K. Singh, B. Ray, S. Parmar, S. Gosavi, V. Sathe, R. J. Choudhary, S. Datar, S. Ogale, *Phys. Rev. Mater*. 2009, **3**, 074007.

[2] A. S. Bhavya, P. Surendran, H. Varghese, A. Chandran, K. P. Surendran, *Nano Energy* 2021, **90**, 106628.

[3] Z. Yang, X. Zhang, G. Xiang, *ACS Appl. Nano Mater*. 2022, **5**, 16906−16911.

[4] A. S. Bhavya, P. Surendran, H. Varghese, A. Chandran, K. P. Surendran, *ACS Appl. Electron. Mater*. 2023, **5**, 5483−5493.

[5] K. V. Vijoy, Anlin Lazar K., H. John, K. J. Saji, *AIP Conf. Proc*. 2023, **2783**, 040001.

[6] K. Zhao, Z. Gao, J. Zhang, J. Zhou, F. Zhan, L. Qiang, M-J. Liu, R-H. Cyu, Y-L. Chueh, *J. Power Sources* 2024, **614**, 234997.

[7] B. Das, R. Paul, R. Karmakar, A. K. Meikap, A. Kumar, S. Krishnamurthy, R. Ghosh, *ACS Appl. Energy Mater*. 2024, **7**, 7025−7036.